Chemical Engineering Journal xxx (xxxx) xxx–xxx

Contents lists available at ScienceDirect

Chemical Engineering Journal

journal homepage: www.elsevier.com/locate/cej

Development of a flat membrane microchannel packed-bed reactor for scalable aerobic oxidation of benzyl alcohol in flow

Gaowei Wu[a], Enhong Cao[a], Peter Ellis[b], Achilleas Constantinou[a,1], Simon Kuhn[a,2], Asterios Gavriilidis[a,*]

[a] Department of Chemical Engineering, University College London, Torrington Place, London WC1E 7JE, UK
[b] Johnson Matthey Technology Centre, Blounts Court, Sonning Common, Reading RG4 9NH, UK

HIGHLIGHTS

- A membrane catalytic packed-bed reactor was designed for safe scalable alcohol oxidation.
- The reactor performance was affected by the oxygen supply.
- The main oxygen transfer resistance was in the bulk liquid within the bed.
- An effectiveness factor was proposed to aid membrane reactor design.

GRAPHICAL ABSTRACT

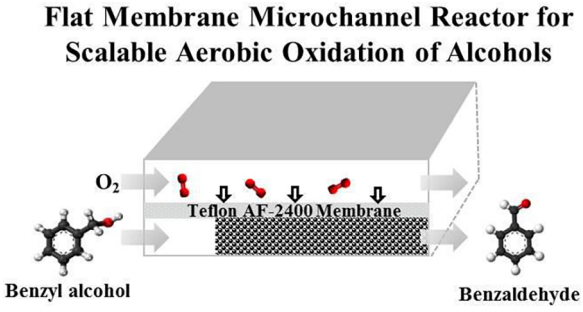

ARTICLE INFO

Keywords:
Gold-palladium catalyst
Teflon AF-2400 membrane
Membrane microchannel reactor
Aerobic oxidation of alcohol
Effectiveness factor

ABSTRACT

A flat membrane microchannel reactor was designed and demonstrated for the safe and scalable oxidation of solvent-free benzyl alcohol with molecular oxygen on Au-Pd/TiO_2 catalyst. The microchannel reactor employed a mesh-supported Teflon AF-2400 membrane, with gas and liquid channels on each side. Catalyst particles were packed in the liquid flow channel. Operation with 20 bara pressure difference between the gas and the liquid phases was possible at 120 °C. Pervaporation of organics through the membrane was experimentally measured to ensure that the organic vapour concentration remained below the lower flammability limit during the reaction. High oxygen pressure was shown to have a positive effect on reactor performance. A conversion of benzyl alcohol of 70% with 71% selectivity to benzaldehyde was obtained at 1150 g_{cat}·s/$g_{alcohol}$, 8.4 bara oxygen pressure and 10 bara liquid pressure. The oxygen consumption rate was not significantly decreased when doubling the membrane thickness, indicating that the membrane generated only low resistance to oxygen mass transfer. When changing the catalyst particle size and the liquid flow rate, no significant effect was observed on the oxidation reaction rate. An effectiveness factor approach is proposed to assess the effect of oxygen permeation and transverse mass transfer on the catalyst packed in the membrane reactor, which suggests that the oxidation of benzyl alcohol on the highly active Au-Pd/TiO_2 catalyst is controlled by the oxygen transverse mass transfer in the bulk liquid within the catalyst bed. Scale-up of the flat membrane microchannel reactor was demonstrated through increasing the liquid channel width by approximately ten times, which increased the reactor productivity by a factor of eight.

* Corresponding author.
E-mail address: a.gavriilidis@ucl.ac.uk (A. Gavriilidis).
[1] Current address: Division of Chemical and Petroleum Engineering, School of Engineering, London South Bank University, 103, Borough Road, London SE1 0AA, UK.
[2] Current address: Department of Chemical Engineering, KU Leuven, Celestijnenlaan 200F, 3001 Leuven, Belgium.

https://doi.org/10.1016/j.cej.2018.10.023

Nomenclature

Bi	Biot number [-]
C	concentration [mol/m^3]
CCT	catalyst contact time [g_{cat}·min/$g_{alcohol}$]
Da	Damköhler number [-]
$D_{O2,T}$	transverse dispersion coefficient of oxygen in the packed bed [m^2/s]
d_1	depth of the packed bed [m]
F	molar flow rate [mol/min]
k_m	oxygen mass transfer coefficient in the membrane [m/s]
k_{O2}	oxidation reaction rate constant based on bed volume [s^{-1}]
m_{cat}	mass of catalyst [mg]
n_{metal}	moles of metals contained in the catalyst bed [mol]
OCR	oxygen consumption rate [mL/min]
TOF	turnover frequency [h^{-1}]
S	selectivity [%]
$\tilde{V}_{O2}$	molar volume of oxygen at standard temperature and pressure [mL/mol]
X	conversion of benzyl alcohol [%]

Greek Symbols

η	permeation-transverse mass transfer effectiveness factor [-]
ν	number of moles of benzyl alcohol consumed for the production of 1 mol of product i [-]
ρ	density [g/mL]
υ	volumetric flow rate of benzyl alcohol [μL/min]

Subscripts

B	benzaldehyde
$BnOH$	benzyl alcohol
D	disproportionation reaction
i	benzaldehyde, toluene
in	inlet of the reactor
O	oxidation reaction
O_2	oxygen
out	outlet of the reactor
T	toluene or transverse
$total$	overall reaction

1. Introduction

Oxidation of alcohols is an important process in organic chemistry and is often performed with stoichiometric inorganic reagents [1–3]. To improve the atom efficiency and reduce the environmental costs, heterogeneous catalysts have been developed, and significant advances have been reported [4–8]. However, large-scale applications of aerobic oxidation of alcohols are still limited by potential safety issues caused by the oxidant-organic reactant mixtures [5,9,10].

Recently, several approaches have been proposed to ensure intrinsic process safety [11]. Stahl and co-workers [12,13] reported a continuous flow tube reactor for homogeneous Pd-/Cu-catalyzed aerobic oxidation of primary alcohols to aldehydes, where a dilute oxygen source (8–9% oxygen in nitrogen) was used to avoid the oxygen/organic mixture entering the flammable regime. Zotova et al. [14] developed a safe process for aerobic oxidation of alcohols with a commercially available XCube™ reactor, by pre-mixing and saturating the liquid with the gaseous reactant (oxygen or air) before reaching the catalyst bed.

Among these approaches, membrane reactors have attracted attention, since a membrane can act as a well-defined contacting interface for gas and liquid phases [15–17]. The membrane allows strict dosing control of gaseous reactants and avoids direct mixing of oxygen with organic compounds. A ceramic membrane reactor was previously developed by our group for oxidation of benzyl alcohol with pure oxygen [18]. The reactor consisted of a commercially available tubular ceramic membrane with catalyst packed in the inner tube. The liquid phase flowed through the inner tube and pure oxygen flowed in the opposite side of the membrane. Deficiency of oxygen in the catalyst bed area was suggested to occur for the relatively fast catalytic system investigated.

As a type of amorphous fluoroplastic, Teflon AF-2400 has gained popularity, since it has high permeabilities to gases and excellent chemical compatibility [19]. The Ley group first developed a Teflon AF-2400 tube-in-tube membrane reactor and applied it to various reactions such as C–C, C–N and C–O bond forming and hydrogenation reactions [20,21]. Chaudhuri et al. [22] used the tube-in-tube reactor to saturate the liquid stream with oxygen/air for heterogeneously catalytic oxidation of alcohols. An *in-situ* continuous supply of oxygen through the membrane to the catalyst was realized through packing the solid catalyst inside the inner tube of the tube-in-tube reactor [23]. This contributed to a significant improvement in both conversion and selectivity, as compared to a nonpermeable reactor with oxygen presaturated feed. Greene et al. [24] developed a tube-in-shell membrane reactor with inexpensive PTFE tubing for homogeneous and heterogeneous oxidation of alcohols with molecular oxygen. Even though the price of common fluoropolymers, such as PTFE, is much lower than that of Teflon AF-2400, the high oxygen permeability of the Teflon AF-2400 membrane makes it attractive for oxidation of solvent-free benzyl alcohol within a catalyst bed.

Some potential drawbacks still exist for the packed tube-in-tube membrane reactor. The gas phase present in the annulus between the inner and outer tubes could possibly create heat transfer resistance for exothermic reactions, due to its relatively low thermal conductivity. The scale-up of the tube-in-tube reactor is not facile, since increasing the membrane diameter results to a proportional increase in radial mass transfer resistance under laminar flow [25]. In an attempt to address these issues, a Teflon AF-2400 flat membrane microchannel reactor is developed in this study. Oxidation of benzyl alcohol is performed on Au-Pd/TiO_2 catalyst, which has high activity and good reusability [26]. The reaction is considered to comprise of two main parallel reactions, the oxidation reaction (Eq. (1), $\Delta H = -218$ kJ/mol$_{benzyl\ alcohol}$, adiabatic temperature rise $\Delta T_{ad} = 884$ °C, assuming no phase change) and the disproportionation reaction (Eq. (2), $\Delta H = -25.6$ kJ/mol$_{benzyl\ alcohol}$, $\Delta T_{ad} = 127$ °C) [27,28]. Both the oxidation and disproportionation of benzyl alcohol can form the target product benzaldehyde, while the toluene by-product is generated from disproportionation. In our recent microkinetic study, hydrogenolysis of benzyl alcohol to toluene was found to play an important role for toluene formation, but at oxygen deficient conditions disproportionation prevails [29]. Hence, in our discussions in this work the hydrogenolysis pathways are neglected, since in the packed-bed membrane reactor (as will be shown) there is deficiency of oxygen supply. The amount of consumed oxygen during the reaction could be calculated based on the conversion of benzyl alcohol and selectivities to benzaldehyde and toluene [23].

$$2PhCH_2OH + O_2 \rightarrow 2PhCHO + 2H_2O \quad (1)$$

$$2PhCH_2OH \rightarrow PhCHO + PhCH_3 + H_2O \quad (2)$$

2. Experimental section

2.1. Catalyst preparation

A nominal 1 wt% bimetallic Au-Pd/TiO_2 catalyst was prepared by co-impregnation, similar to previous work [26,30]. TiO_2 (Degussa, P25) was first suspended in demineralized water by stirring, and then

$HAuCl_4{\cdot}3H_2O$ (Johnson Matthey) and $PdCl_2$ (Johnson Matthey) with Au-to-Pd weight ratio equivalent to 1:19 was added. The resultant slurry was spray-dried (nozzle temperature 220 °C) and then calcined in static air at 400 °C for 1 h. The metal content was analysed by ICP-AES and found to be 0.05 wt% Au and 0.85 wt% Pd, while the metal particle size as observed by TEM was 1–2 nm. The powder was pelletized, crushed, and sieved to the desired particle size range. The shape of the catalyst particles, as observed with a microscope, was irregular (shown in Fig. S1) and the particle density, as calculated from the skeletal density and the pore volume (measured by BET), was 2.19 g/cm^3.

2.2. Design of the flat membrane microchannel reactor

The flat membrane microchannel reactor designed in this work consisted of several layers, which are shown in Fig. 1. From the bottom to the top, these are a liquid flow plate machined in 316 stainless steel (channel size length: 75 mm; width: 3 mm; depth: 1 mm), a Teflon AF-2400 membrane (length: 85 mm; width: 30 mm; thickness: 0.07 mm; Biogeneral), a 304 stainless steel mesh (length: 85 mm; width: 30 mm; thickness: 0.05 mm; hole size: 76 µm; open area: 23%; Industrial Netting; shown in Fig. S2), viton gasket (length: 85 mm; width: 30 mm; thickness: 1 mm; open area length: 75 mm; width: 3 mm; Altec) and a gas flow plate (with the same channel size and material to the liquid flow plate). The sealing of the reactor was achieved by compressing the membrane and the gasket with screws; the membrane also acted as a gasket for the liquid flow plate. An O-ring groove was machined in the liquid flow plate, which allowed also a sintered metal plate to be employed as the membrane support. Two holes were drilled in both liquid and gas channel plates (perpendicular, 1 mm away from the channel) for thermocouple insertion. A small circular piece of another nickel mesh (diameter: ~2 mm; thickness: 0.05 mm; hole size: 25 µm; Tecan) was placed between the liquid outlet and the fitting for retaining the catalyst. After assembling the reactor, 50 mg silica beads (particle size: 90–125 µm) were packed into the liquid channel followed by the Au-Pd/TiO_2 catalyst particles, with the help of a vacuum pump. For the 90–125 µm particles, the length of the 100 mg catalyst bed was 4.1 ± 0.2 cm, and the packing density was ~0.82 g/cm^3, leading to a void fraction of the catalyst bed of 0.62.

The reactor was placed on a hotplate (Gallenkamp) fitted with a thermocouple which was inserted in the liquid flow plate hole beneath the catalyst bed for temperature measurement and control. To decrease heat loss, an insulation cap (insulation thickness: ~2 cm; WDS® Ultra, Morgan) was made to cover the reactor. The temperature difference between the gas and the liquid flow plates during the reaction at 120 °C measured with the thermocouples was < 3 °C.

2.3. Scale-up of the flat membrane microchannel reactor

To scale-up the reactor, the gas and liquid channel widths were increased to 32 mm. CFD modelling was performed with COMSOL Multiphysics® Modelling Software (using the Navier-Stokes and the continuity equations) to ensure proper flow distribution (the simulation results are shown in the Supporting Information). The gas flow channels were 1 mm deep, and pillars and fins were designed to distribute the gas flow and assist in supporting the membrane. The length of the liquid flow channel was 68 mm, with a depth of 0.5 mm. Distribution channels were machined at the inlet and outlet of the liquid flow plate. Sintered metal filters (304 stainless steel; Mott, grade 0.1) were inserted between the liquid distribution channels and the liquid channel to retain the catalyst particles. To better seal the top edge of the catalyst filters, a Kalrez® gasket (thickness: 0.5 mm; DuPont™) was added between the liquid flow plate and the membrane, which also made the total depth of liquid channel (machined liquid channel plus open area of the Kalrez® gasket) close to 1 mm. The catalyst was packed in the liquid flow channel through an opening (diameter: 2 mm) that was drilled on one side of the liquid flow plate.

The scaled-up reactor was heated with two silicone rubber heaters (Watlow, wire-wound elements 020050C2). The whole reactor was insulated by an insulation cap (insulation thickness: ~2 cm; WDS® Ultra, Morgan) and the temperature difference within the reactor, measured by thermocouples inserted in liquid flow plate holes close to the flow channels, was ± 2 °C at set temperature of 120 °C.

2.4. Reaction experiments

A schematic of the experimental set-up is shown in Fig. 2. Neat benzyl alcohol (99.0%, Sigma-Aldrich) was delivered to the microchannel reactor with a HPLC pump (Knauer P2.1S). An adjustable back pressure regulator (BPR) (Zaiput, BPR-01) was used at the liquid outlet to maintain the desired liquid pressure. Pure oxygen was regulated by a mass flow controller (Brooks, GF40 series) and directed to the gas inlet of the reactor. A BPR (1–11 bara, Swagelok, K series) was connected at the gas outlet to maintain the desired gas pressure. The pressures of the gas and liquid phases were monitored by pressure sensors (Zaiput, Hastelloy/PFA wetted parts) placed ~20 cm from the inlets of the reactor. The packed bed pressure drop was measured to be less than 0.2 bara. To avoid bubble formation in the liquid phase, the inlet pressure of the liquid phase was maintained at least 1 bara higher than that of the gas phase pressure.

The effluent from the liquid outlet was collected in a cold trap (ice-water bath) and quantitatively analysed by a gas chromatograph (Agilent 7820A) fitted with a DB-624 capillary column and a flame ionization detector. Benzyl alcohol conversion (X) and selectivity (S_i) of each product were calculated according to the following equations:

$$X = \frac{C_{BnOH,in} - C_{BnOH,out}}{C_{BnOH,in}} \tag{3}$$

$$S_i = \frac{C_i \cdot \nu_i}{C_{BnOH,in} \cdot X} \tag{4}$$

where $C_{BnOH,in}$ and $C_{BnOH,out}$ are the concentration of benzyl alcohol at the inlet and outlet of the reactor, respectively and ν_i is the number of moles of benzyl alcohol consumed for the production of 1 mol of product i. In this study, S_B and S_T stand for selectivities to benzaldehyde and toluene, respectively.

The catalyst contact time (CCT) was used to characterise the reaction time of benzyl alcohol, and defined as:

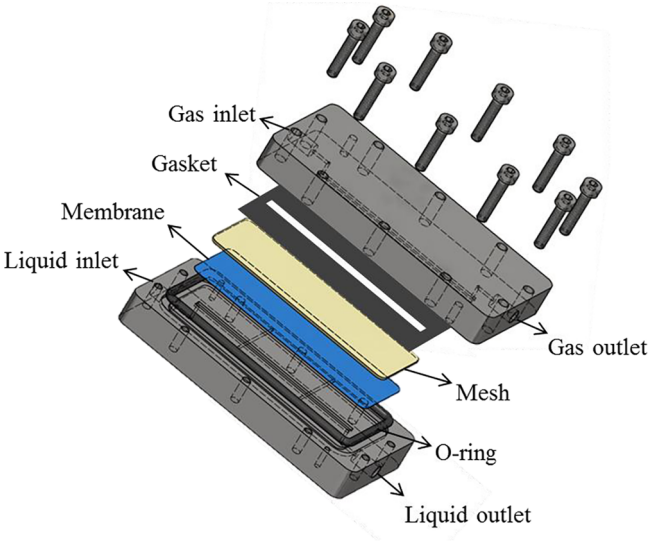

Fig. 1. Schematic of the flat membrane microchannel reactor consisting of gas and liquid flow plates with viton gasket, stainless steel mesh, and Teflon AF-2400 membrane.

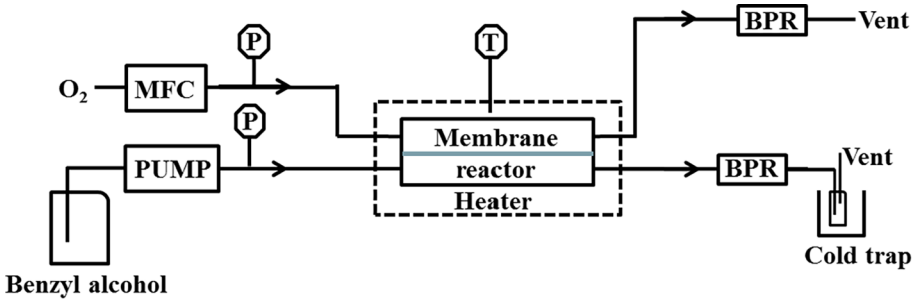

Fig. 2. Schematic of the flat membrane microchannel reactor set-up (MFC: mass flow controller; P: pressure sensor; T: thermocouple; BPR: back pressure regulator).

$$CCT = \frac{m_{cat}}{\upsilon\rho} \tag{5}$$

where m_{cat} is the mass of catalyst, υ is the inlet volumetric flow rate of benzyl alcohol, ρ is the density of benzyl alcohol at 20 °C. For each experiment, at least three samples were collected and the results were averaged. The experimental errors for the conversion and selectivities were less than ± 2% (absolute). For typical operating conditions (catalyst contact time, 577 g_{cat}·s/$g_{alcohol}$; oxygen pressure, 8.4 bara; liquid pressure, 10 bara; 120 °C) the conversion and selectivities obtained in different days could differ by up to 4% (absolute), primarily due to a slow catalyst deactivation. Oxygen consumption rates (*OCR*, at standard temperature and pressure, 0 °C and 1 bara, STP) were calculated by

$$OCR = \frac{1}{2}\cdot F_{BnOH,in}\cdot X\cdot(S_B - S_T)\cdot\tilde{V}_{O2} \tag{6}$$

where $F_{BnOH,in}$ is the molar flow rate of benzyl alcohol and $\tilde{V}_{O2}$ is the molar volume of oxygen at STP.

Average turnover frequency (*TOF*) was calculated to better represent the reaction rate, where TOF_{total}, TOF_O and TOF_D correspond to the overall reaction, the oxidation reaction and the disproportionation reaction, respectively.

$$TOF_{total} = \frac{F_{BnOH,in}\cdot X}{n_{metal}} \tag{7}$$

$$TOF_O = \frac{F_{BnOH,in}\cdot X\cdot(S_B - S_T)}{n_{metal}} \tag{8}$$

$$TOF_D = \frac{2F_{BnOH,in}\cdot X\cdot S_T}{n_{metal}} \tag{9}$$

where n_{metal} is the moles of the metals contained in the packed catalyst bed.

3. Results and discussion

3.1. Operation pressure and solvent pervaporation

Initially, the operating pressure range of the reactor was studied without any catalyst packed. The reactor temperature was kept at 120 °C and atmospheric pressure was applied in the gas phase. The pressure in the liquid phase was gradually increased to 21 bara (20 bara pressure difference) and kept for 0.5 h. No leaking was detected. Noticably, only slight change of the shape of the membrane was observed after testing at such pressure difference and temperature (shown in Fig. S4a). In contrast, obvious membrane shape change was observed when no mesh was used to support the membrane (shown in Fig. S4b). However, membrane shape change was restricted and breakage was prevented, because the membrane eventually touched the bottom of the gas channel with increasing liquid pressure. It should be noted that in our previous tube-in-tube membrane microreactor, the Teflon AF-2400 inner tube (1 mm thickness) broke when ~12 bara pressure difference was applied at 120 °C. This indicates that the flat membrane microchannel reactor could expand the operating pressure range of the Teflon AF-2400 membrane at elevated temperature.

Even though direct mixing of oxygen with organic reactants is avoided by using the membrane reactor, organic vapour may appear in the gas phase because of pervaporation. To ensure that the organic vapour concentration remained outside the flammability limits, the pervaporation of the reactant and the main products (benzyl alcohol, benzaldehyde and toluene) through the membrane was experimentally measured and the details are shown in the Supporting Information. The pervaporation rate of toluene through the membrane was found to be the highest, which was 32.2 mg/h (for 14.3 mg/h/cm^2 membrane area). This corresponded to 0.13 mL/min toluene vapour in the gas phase channel at STP, highlighting the necessity of using continuous flow in the gas phase to dilute the pervaporating organics. To keep the organic vapour concentration lower than 1 vol% (which is the lower flammability limit for toluene in air at 6 bara and 120 °C [31]), an oxygen flow rate of 15 mL/min at STP was utilized in the following experiments.

3.2. Catalyst stability

To evaluate the performance of the Au-Pd/TiO_2 catalyst and the reactor, a stability study was initially conducted and the results are shown in Fig. 3. The catalyst contact time was 577 g_{cat}·s/$g_{alcohol}$ and the conversion of benzyl alcohol was stable at around 57% over 24 h. The selectivities to benzaldehyde and toluene, the two main products, also showed stable trends (66% and 31%, respectively). The selectivities to other minor products (dibenzyl either, benzyl benzoate, *etc.*) were all less than 3% (not shown). These results demonstrate the high stability of the prepared Au-Pd/TiO_2 catalyst, as well as the excellent performance of the flat membrane microchannel reactor. The productivity of benzaldehyde was calculated to be 2.3 g_B/(g_{cat}·h).

3.3. Effect of oxygen pressure

To explore the effect of oxygen pressure on the oxidation of benzyl alcohol in the flat membrane microchannel reactor, oxygen pressure was changed from 0 to 8.4 bara. Other reaction conditions were kept the same. From Fig. 4, the conversion of benzyl alcohol was observed to be 4% at 0 bara oxygen pressure (nitrogen flowed through the gas channel at atmospheric pressure). Almost equimolar amounts of benzaldehyde (44%) and toluene (41%) were formed due to the disproportionation of benzyl alcohol [27,28,32]. With oxygen pressure increasing, the conversion gradually rose and reached 57% at 8.4 bara. The selectivity to benzaldehyde also increased from 44% to 66% within the investigated oxygen pressure range. Correspondingly, the selectivity to toluene drop from 41% to 31%. Similar behaviour was also observed in our previous tube-in-tube membrane microreactor [23]. When increasing the oxygen pressure from 3 to 7 bara, the conversion of benzyl alcohol increased from 22% to 42% with the selectivity to benzaldehyde from 61% to 65% at catalyst contact time 115 g_{cat}·s/$g_{alcohol}$.

The oxygen consumption rate at STP under different oxygen pressures is shown in Fig. 5. Higher oxygen consumption rates were

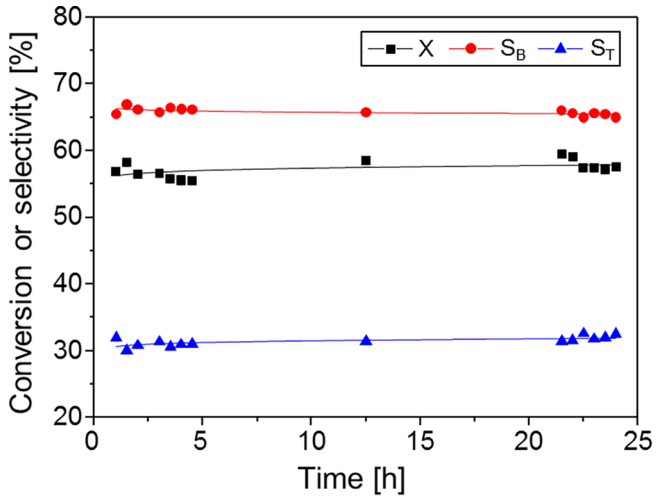

Fig. 3. Conversion of benzyl alcohol, X, and selectivities to benzaldehyde, S_B, and toluene, S_T, as a function of operation time. Reaction conditions: Au-Pd/TiO_2 catalyst (90–125 μm), 100 mg; neat benzyl alcohol, 10 μL/min; catalyst contact time, 577 g_{cat}·s/$g_{alcohol}$; oxygen pressure, 8.4 bara; liquid pressure, 10 bara; reaction temperature, 120 °C.

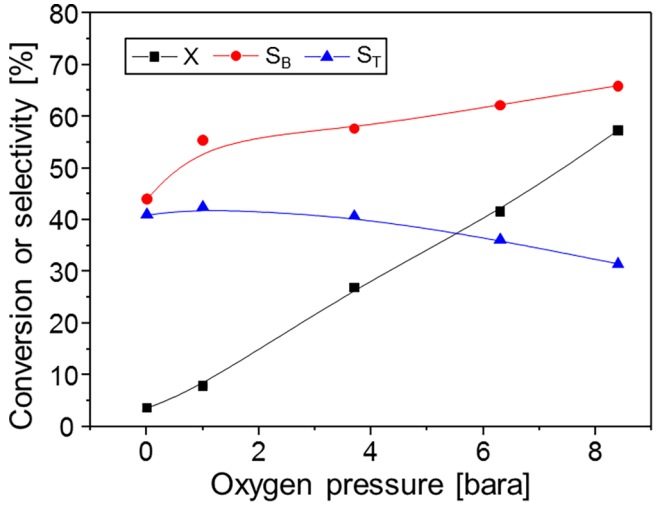

Fig. 4. Effect of oxygen pressure on the conversion of benzyl alcohol, X, and selectivities to benzaldehyde, S_B, and toluene, S_T. Reaction conditions: Au-Pd/TiO_2 catalyst (90–125 μm), 100 mg; neat benzyl alcohol, 10 μL/min; catalyst contact time, 577 g_{cat}·s/$g_{alcohol}$; liquid pressure, 10 bara; reaction temperature, 120 °C.

observed at higher gas pressure. The maximum rate was 0.21 mL/min (STP, 0.56 mmol/h) at 8.4 bara. The fact that the oxygen consumption rate was close to zero at 0 bara oxygen pressure (nitrogen was used in the gas channel), indicates that the amount of oxygen consumed in the reaction at elevated oxygen pressure comes from oxygen permeating through the membrane during the reaction. On the basis that all other reaction conditions were kept the same and only the oxygen pressure was changed, increasing the oxygen pressure could therefore enhance the oxygen consumption and result in higher oxygen permeation.

To further investigate the effect of oxygen pressure on the reaction, TOFs at different oxygen pressures were calculated and shown in Fig. 6. In the absence of oxygen (0 bara oxygen pressure), TOF_{total} was very close to TOF_D, and TOF_O was practically zero. This indicates that disproportionation was the only reaction occurring and no oxidation reaction was taking place under these conditions [28]. With a rise in oxygen pressure, both TOF_D and TOF_O showed an upward monotonic trend. This contributed to an approximately linear increase in TOF_{total}, as well as the increasing selectivity to benzaldehyde as shown in Fig. 4. Since the oxygen solubility in the liquid increases at elevated oxygen pressure, this demonstrates that oxygen could promote both disproportionation and oxidation reactions. This has been observed previously and has been attributed to two different mechanisms for the disproportionation reaction, one anaerobic and the other aerobic [27,28,33]. At low oxygen pressure the anaerobic route dominates, but an increase of oxygen concentration promotes the aerobic disproportionation route, which has been associated with oxygen regenerating the active sites for the disproportionation reaction [28]. Higher TOF_{total} and TOF_O were observed in batch reactors and microtrickle bed reactors, when higher oxygen pressure was used. However, the TOF_D in both batch and microtrickle bed reactors was observed to decrease with oxygen pressure higher than 0.2–1 bara [27,33], indicating the dominance of the oxidation reaction (as compared to both aerobic and anaerobic disproportionation) at high oxygen concentration. The detailed description of the proposed mechanism for the anaerobic and aerobic disproportionation can be found in [27,28]. The fact that TOF_D in the membrane reactor was not observed to decrease within the range of oxygen pressures investigated, suggests that the reactor might not supply oxygen as efficiently as the batch and trickle bed reactors. The low oxygen supply in the membrane reactor is also indicated by the obtained TOFs, since the TOFs in the membrane reactor (TOF_{total}, 400 h^{-1} at 8.4 bara) were about two orders of magnitude lower than those reported in batch reactors using 2.5 wt% Au-2.5 wt% Pd/TiO_2 catalyst (TOF_{total}, 26,400 h^{-1}) [26]. So, in the following sections the oxygen transfer resistance in the reactor was investigated.

3.4. Effect of catalyst contact time and membrane thickness

The effect of membrane thickness was investigated through placing a single-layer (0.07 mm thickness) or a double-layer (0.14 mm thickness) membrane in the microchannel reactor. The results at different catalyst contact times are shown in Fig. 7. The same trend was observed for the conversion and selectivities at different catalyst contact times, that is, increasing the catalyst contact time enhanced both the conversion of benzyl alcohol and the selectivity to benzaldehyde, while decreasing the selectivity to toluene. This trend agrees with our previous results in the membrane reactors [18,23], but differs from those obtained in batch and trickle bed reactors [28,32], in which the selectivities were similar at different catalyst contact times. This is

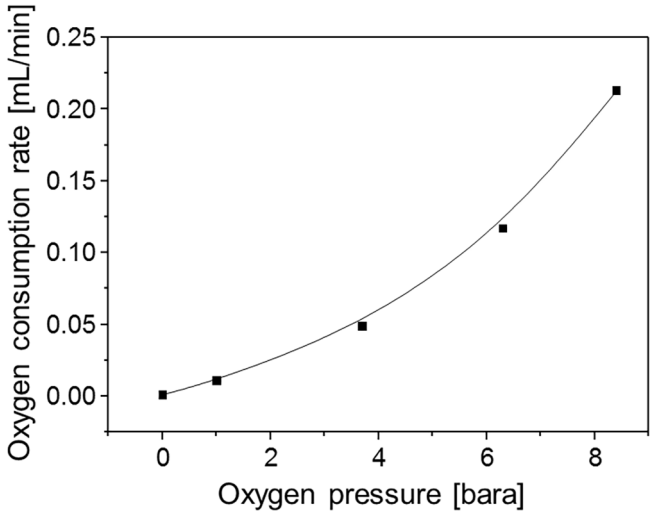

Fig. 5. Oxygen consumption rates at STP at different oxygen pressures. Reaction conditions: Au-Pd/TiO_2 catalyst (90–125 μm), 100 mg; neat benzyl alcohol, 10 μL/min; catalyst contact time, 577 g_{cat}·s/$g_{alcohol}$; liquid pressure, 10 bara; reaction temperature, 120 °C.

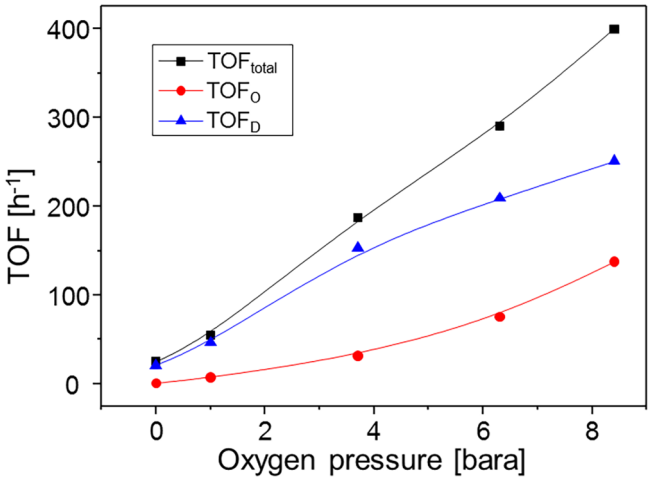

Fig. 6. Average turnover frequencies at different oxygen pressures. Reaction conditions: Au-Pd/TiO_2 catalyst (90–125 μm), 100 mg; neat benzyl alcohol, 10 μL/min; catalyst contact time, 577 g_{cat}·s/$g_{alcohol}$; liquid pressure, 10 bara; reaction temperature, 120 °C.

probably caused by the low efficiency of oxygen supply in the membrane reactors as discussed in Section 3.3. Longer catalyst contact time in the membrane reactor could contribute to longer time for both oxygen permeation and reaction, and thus more oxygen supply per liquid volume [23]. This could further promote the oxidation reaction, resulting in benzaldehyde selectivity increase.

Notably, a conversion of benzyl alcohol of 70% with 71% selectivity to benzaldehyde was obtained at 1150 g_{cat}·s/$g_{alcohol}$ and 8.4 bara oxygen pressure with a single-layer membrane. At the same reaction conditions with double-layer membrane, the conversion and benzaldehyde selectivity were observed to be both 68%. When comparing the oxygen consumption rates at different membrane thicknesses (shown in Fig. 7c), higher rate was observed for the single-layer membrane at each catalyst contact time. The average oxygen consumption rate with the single-layer membrane (0.19 mL/min) was 27% higher than that with the double-layer (0.15 mL/min). This reveals that some oxygen transfer resistance exists in the membrane. However, the oxygen transfer resistance in the membrane does not seem to be the main transfer resistance, since only 27% increase of average oxygen consumption rate was observed when halving the membrane thickness.

3.5. Internal/external mass transfer

The internal mass transfer was studied using two ranges of catalyst particle sizes at different catalyst contact times. The conversion of benzyl alcohol and selectivities to benzaldehyde and toluene are shown in Fig. 8. Slightly higher conversion was observed when larger particles were used. This is attributed to slightly longer packed bed obtained with larger particles for the same catalyst weight (packed bed length: 4.1 ± 0.2 cm for 90–125 μm particles vs. 3.5 ± 0.2 cm for 45–53 μm particles), which led to increasing the membrane area available for oxygen transfer without increasing the oxygen demand by the catalytic bed. A similar effect has been observed when the catalyst bed was diluted with inert support [23]. The selectivities to benzaldehyde and toluene were similar, indicating independence on the catalyst particle size. Simplified calculation of the Weisz-Prater criterion (see Supporting Information) indicated small diffusional resistances, but due to the unknown (and likely transversely and axially varying) oxygen concentration within the catalyst bed, the criterion cannot be used reliably. However, the results with the two catalyst particle sizes indicate that internal mass transfer resistance is not a determining factor for the performance of the system investigated.

The external mass transfer was studied by comparing the TOFs for

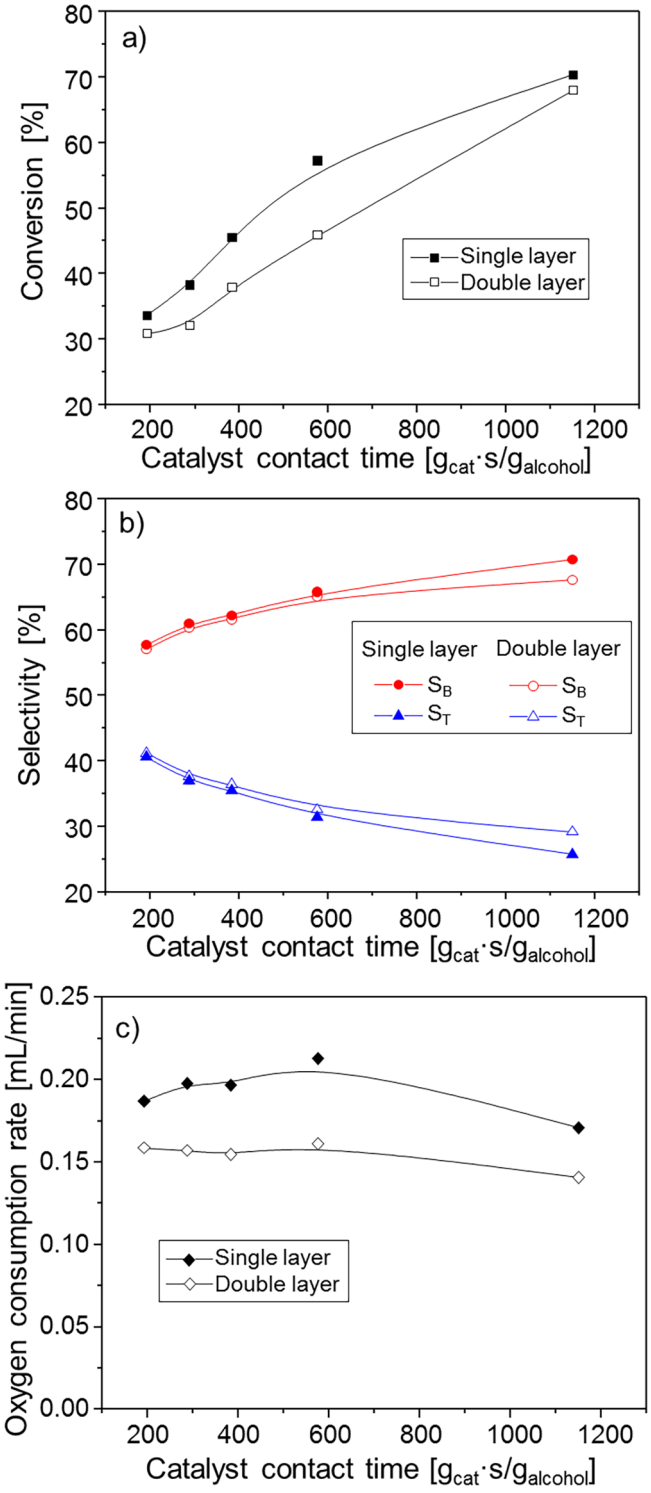

Fig. 7. Effect of membrane thickness on the conversion of benzyl alcohol, selectivities to benzaldehyde, S_B, and toluene, S_T, and oxygen consumption rate. Single layer membrane, 0.07 mm; double layer membrane, 0.14 mm. Reaction conditions: Au-Pd/TiO_2 catalyst (90–125 μm), 100 mg; neat benzyl alcohol, 5–30 μL/min; oxygen pressure: 8.4 bara; liquid pressure, 10 bara; reaction temperature, 120 °C.

two different liquid flow rates at three catalyst contact times. The amount of catalyst packed in the reactor was changed accordingly. Note that these are average TOFs obtained at conversion levels 30–60%. In Table 1, no clear difference was seen in all the TOFs, when the liquid flow rate was increased from 5 μL/min to 10 μL/min at 577 g_{cat}·s/

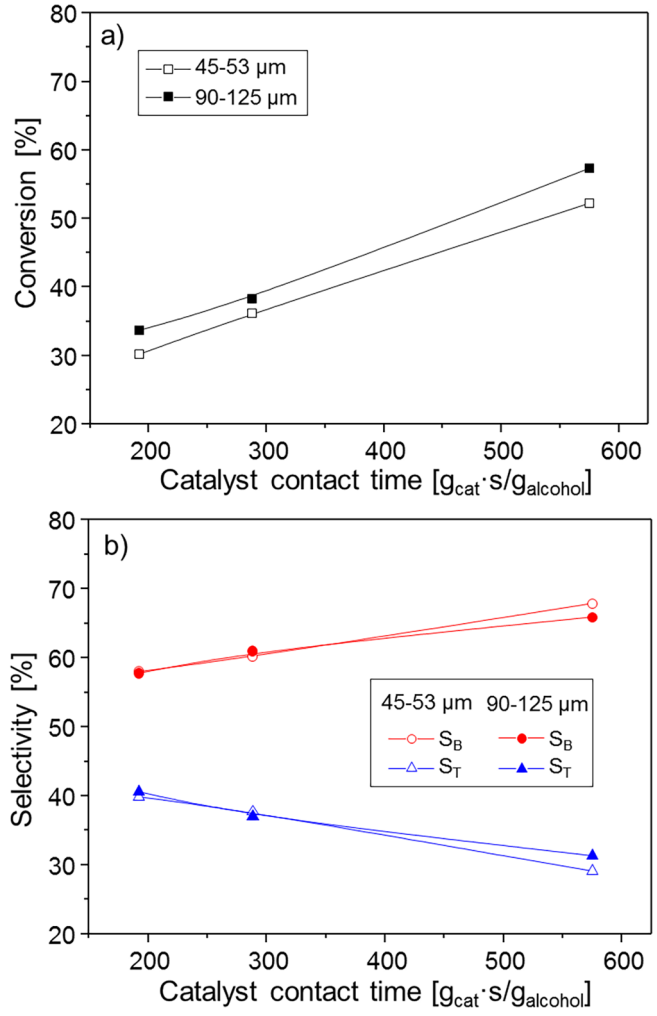

Fig. 8. Effect of catalyst particle size on the conversion of benzyl alcohol and selectivities to benzaldehyde, S_B, and toluene, S_T. Reaction conditions: Au-Pd/TiO_2 catalyst, 100 mg; oxygen pressure: 8.4 bara; liquid pressure, 10 bara; reaction temperature, 120 °C.

$g_{alcohol}$. When liquid flow rate was increased from 10 μL/min to 20 μL/min at shorter catalyst contact time (288 g_{cat}·s/$g_{alcohol}$), TOF_{total} increased by 14%. This is caused by the increase of TOF_D (24%), despite the slight decrease in TOF_O. Higher increase of TOF_{total} (28%) was observed with liquid flow rate increasing from 15 μL/min to 30 μL/min at 192 g_{cat}·s/$g_{alcohol}$. A rise of 43% was also observed in TOF_D, together with 12% drop in TOF_O. The small decreases of TOF_O with higher flowrate is counterintuitive and could possibly be caused by different catalyst packing and some catalyst deactivation. However, the changes of TOF_D illustrate stronger influence of the liquid flow rate on the disproportionation reaction than the oxidation reaction.

The flat membrane microchannel reactor has been indicated not to supply oxygen as efficiently as the batch and microtrickle bed reactors (see Sections 3.3 and 3.4). Note that the direction of oxygen transfer in the membrane reactor is perpendicular to that of liquid flow (in laminar flow regime), and oxygen needs to permeate the membrane, dissolve in the liquid, transfer transversely through the bulk liquid within the catalyst packed bed and reach the catalyst surface. Different liquid flow rates could potentially affect both the external mass transfer and the transverse mass transfer of oxygen in the bed, and thus affect the oxygen supply to the catalyst. The stronger influence of liquid flow rate on the disproportionation reaction, rather than the oxidation reaction, can be due to the dominance of the disproportionation reaction at low oxygen supply (as discussed in Section 3.3).

Based on the TOF_{total} (26,400 h^{-1}) and the selectivity to benzaldehyde (~67%) obtained with 2.5 wt% Au-2.5 wt% Pd/TiO_2 catalyst in a batch reactor [26], the TOF_O of the Au-Pd/TiO_2 catalyst was calculated to be ~8800 h^{-1} at 120 °C. This results to an oxygen demand of 13.6 mL/min at STP (36.5 mmol/h, calculation shown in the Supporting Information) for the amount of Au-Pd/TiO_2 catalyst packed in the membrane reactor (100 mg). The actual oxygen consumption rate within the membrane reactor was only 0.21 mL/min (0.56 mmol/h) at 8.4 bara oxygen pressure. This indicates a gap between oxygen demand by the highly active catalyst and oxygen supply in the membrane reactor. However, the maximum oxygen supply rate (the highest oxygen permeation rate) through the membrane area contacting the catalyst bed (~40 mm × 3 mm) could be 0.74 mL/min (2.0 mmol/h) at 8.4 bara oxygen pressure, which is more than 3 times the oxygen consumption rate. This oxygen supply rate could contribute to a theoretical 4.0 mmol/h of benzaldehyde formed through the oxidation reaction (considering a stoichiometry according to Eq. (1) of 2/1: benzyl alcohol/oxygen), which is much larger than the actual 1.1 mmol/h. The difference between the maximum oxygen supply rate and the actual oxygen consumption rate indicates oxygen transfer resistance in the catalyst bed. Since the internal/external mass transfer resistance have been shown to have no significant effect on the oxidation reaction rate, the main oxygen transfer resistance is thus expected to exist in the bulk liquid within the catalyst bed.

3.6. Interaction of mass transfer processes with reaction in the packed bed membrane reactor

In order to assess the relative importance of the various mass transfer processes that affect reactor performance (membrane oxygen permeation and transverse mass transfer), a permeation-transverse mass transfer effectiveness factor (η) is proposed, based on the oxidation reaction rate (assumed as a first order in oxygen, the details are shown in the Supporting Information). By considering an analogy between our reactor and a single catalyst pellet where diffusion/reaction occurs, where the oxygen mass transfer through the membrane and transverse mass transfer in the reactor bed are analogous to external and internal mass transfer in a pellet respectively, we can use the standard effectiveness factor analysis.

To relate the reaction rate to the transverse mass transfer rate in the packed bed, a Damköhler number (*Da*) is defined by

$$Da = \frac{d_1^2 k_{O2}}{D_{O2,T}} \tag{10}$$

where d_1 is the depth of the packed bed (i.e., liquid channel), k_{O2} is the oxidation reaction rate constant based on the bed volume, $D_{O2,T}$ is the transverse dispersion coefficient of oxygen in the packed bed.

To provide a measure of oxygen permeation rate to oxygen transverse mass transfer rate, a Biot number (*Bi*) is defined by

$$Bi = \frac{d_1 k_m}{D_{O2,T}} \tag{11}$$

Table 1
Comparison of TOFs for different liquid flow rates. Reaction conditions: Au-Pd/TiO_2 catalyst (90–125 μm), 50 or 100 mg; catalyst contact time, 192–577 g_{cat}·s/$g_{alcohol}$; oxygen pressure: 8.4 bara; liquid pressure, 10 bara; reaction temperature, 120 °C.

CCT [g_{cat}·s/$g_{alcohol}$]	577			288			192		
Catalyst weight [mg]	50	100	–	50	100	–	50	100	–
Liquid flow rate [uL/min]	5	10	$\frac{TOF_{10}}{TOF_5}$	10	20	$\frac{TOF_{20}}{TOF_{10}}$	15	30	$\frac{TOF_{30}}{TOF_{15}}$
TOF_{total} [h^{-1}]	386	400	1.03	468	534	1.14	548	704	1.28
TOF_O [h^{-1}]	143	138	0.96	139	128	0.92	137	121	0.88
TOF_D [h^{-1}]	233	251	1.08	318	395	1.24	399	572	1.43

where k_m is the oxygen mass transfer coefficient in the Teflon AF-2400 membrane, and is inversely proportional to the membrane thickness (shown in the Supporting Information) [25].

So, akin to an overall effectiveness factor in terms of internal and external mass transfer in a single pellet [34], a *permeation-transverse mass transfer effectiveness factor* (η) is described by

$$\eta = \frac{sinh\sqrt{Da}}{\sqrt{Da}\,(cosh\sqrt{Da} + \frac{\sqrt{Da}}{Bi} sinh\sqrt{Da})} \quad (12)$$

For the Au-Pd/TiO_2 catalyst in the current flat membrane microchannel reactor, the Biot number is 68.6 (see Supporting Information), which indicates that the oxygen permeation rate in the membrane is much higher than the oxygen transverse mass transfer rate in the packed bed. This results to slight increase of oxygen consumption rate when halving the membrane thickness. Using an estimated first-order reaction rate constant from the batch reactor, the Damköhler number is 5207, which suggests that the oxidation reaction in the membrane reactor is transverse mass transfer-controlled. The permeation-transverse mass transfer effectiveness factor is found to be 0.7%, which agrees with the ratio (1.5%) of the observed TOF_O in the membrane reactor ($\sim 130\ h^{-1}$) to the batch reactor ($\sim 8800\ h^{-1}$).

Since the oxygen transverse mass transfer rate is inversely proportional to the liquid channel depth, reduction in the liquid channel depth is expected to improve the performance of the membrane reactor for oxidation of benzyl alcohol. To confirm this, another reactor was fabricated with half the liquid channel depth (0.5 mm) but the same channel width (3 mm) as compared to the previous design. The amount of packed catalyst was also halved to keep the length of catalyst bed the same. At the same catalyst contact time (577 g_{cat}·s/$g_{alcohol}$) and oxygen pressure (8.4 bara), a 75% conversion of benzyl alcohol with a 67% selectivity to benzaldehyde was obtained in the 0.5 mm channel depth reactor, as compared to 57% conversion and 66% benzaldehyde selectivity in the 1.0 mm channel depth reactor. This demonstrates that the main oxygen transfer resistance exists in the bulk liquid within the catalyst bed.

To predict catalyst performance in the packed bed membrane reactor and guide reactor design, the effectiveness factor is shown as a function of the observable ηDa for various values of Biot number analogous to [34] in Fig. 9, together with the various regimes of possible controlling processes. When the reactor is in the transverse mass transfer controlling regime (as the symbols shown in Fig. 9, corresponding to the reactors with liquid flow channel depths of 1.0 mm (■) and 0.5 mm (●), indicate), decreasing the channel depth decreases the values of Da and Bi, which makes the effectiveness factor move towards the permeation or reaction controlling regime. When the reactor is in the permeation controlling regime, decreasing the membrane thickness increases the value of Bi, which makes the effectiveness factor move towards the reaction or transverse mass transfer controlling regime. Similarly, in the reaction controlling regime, the value of Da will increase if the reaction rate constant increases. This will make the effectiveness factor move towards the permeation or transverse mass transfer controlling regime.

3.7. Performance of the scaled-up membrane reactor

Scale-up of the flat membrane microchannel reactor was carried out through increasing the channel width by ~10 times, and the results obtained with fresh catalysts are shown in Table 2. The reactor was kept vertical and the liquid flowed from top to bottom. As compared to the previous microchannel reactor (channel width, 3 mm), the scaled-up reactor showed a lower conversion of benzyl alcohol with a similar selectivity to benzaldehyde for the same catalyst contact time. The relative drop in conversion of ~17% may be due to flow maldistribution in the wider liquid channel, possibly caused by nonuniform catalyst packing, as well as reduced oxygen flux across the membrane, due to the fins that were added in the gas channel for achieving equal flow distribution and acting also as membrane support. Nevertheless, the benzaldehyde throughput was demonstrated to be increased by a factor of 8 in the scaled-up microchannel reactor.

The effect of liquid flow direction on the performance of the scaled-up microchannel reactor was further investigated with the same (used) catalyst packing. The reactor was kept vertical with liquid flowing from top to bottom (Table 3a), bottom to top (Table 3b), or horizontal with liquid flowing from left to right (Table 3c). As shown in Table 3a, the conversion of benzyl alcohol was slightly lower (~5%) under the same conditions to that in Table 2, which could be caused by a slight catalyst deactivation after ~50 h operation. However, for the three different flow directions, no obvious difference was observed in terms of conversion and selectivities. This indicates that the liquid flow direction has no effect on the liquid distribution within the liquid channel.

Finally, oxidation of benzyl alcohol was carried out with air in the scaled-up flat membrane microchannel reactor, since air is cheaper and easier to use as compared to pure oxygen. As shown in Fig. S6, the conversion of benzyl alcohol was 27%, with a selectivity of 63% to benzaldehyde. For the same reaction conditions with pure oxygen, the conversion and selectivity to benzaldehyde were 65% and 68%, respectively. The different performance in terms of conversion and selectivity was caused by the different partial pressures of oxygen; as discussed earlier, oxygen is beneficial for both conversion and benzaldehyde selectivity. These results highlight the efficiency of using pure oxygen, suggesting that to achieve similar performance with air, higher gas pressure would need to be utilised.

4. Conclusions

A flat Teflon AF-2400 membrane microchannel reactor was developed and applied for continuous flow aerobic oxidation of solvent-free benzyl alcohol on Au-Pd/TiO_2 catalyst. As compared to a previous tube-in-tube membrane microreactor, the flat configuration provides wider operating pressure range and is more amenable to scale up. Both the small-width and the scaled-up reactors investigated in this work behaved isothermally, even though the reaction was highly exothermic. For further scale-up they can be combined with plate heat exchangers to realize the required temperature control. Higher reaction rates and desired product selectivities were observed at higher oxygen pressure, highlighting the importance of high oxygen concentration for this reaction. Study of the various oxygen transfer processes (permeation through membrane, transverse mass transfer in the catalyst bed, internal/external transfer in the catalyst particles) indicated

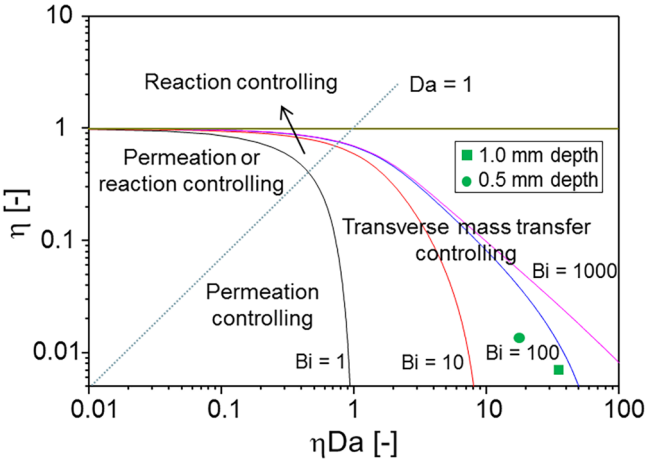

Fig. 9. Permeation-transverse mass transfer effectiveness factor (η) as a function of the observable η*Da* for various values of Biot number (Bi) with the various regimes of possible controlling processes. (Symbols indicate the values for the membrane reactors used with liquid flow channel depth of 1.0 mm (■) and 0.5 mm (●)).

Table 2
Comparison of reactors with different channel width in terms of conversion of benzyl alcohol, X, and selectivities to benzaldehyde, S_B, and toluene, S_T. Reaction conditions: Au-Pd/TiO_2 catalyst (90–125 μm); catalyst contact time, 1150 g_{cat}·s/$g_{alcohol}$; liquid pressure, 10 bara; reaction temperature, 120 °C.

Reactor	Channel width [mm]	Catalyst packed [g]	Liquid flow rate [μL/min]	Oxygen pressure [bara]	X [%]	S_B [%]	S_T [%]
Small	3	0.1	5	8.4	70	71	26
Large	32	1.0	50	8.2	58	69	26

Table 3
Effect of liquid flow direction on the performance of the scaled-up microchannel reactor, in terms of conversion of benzyl alcohol, X, and selectivities to benzaldehyde, S_B, and toluene, S_T. Reaction conditions: Au-Pd/TiO_2catalyst (90–125 μm), 1.0 g; liquid flow rate, 50 μL/min; catalyst contact time, 1150 g_{cat}·s/$g_{alcohol}$; oxygen pressure, 8.2 bara; liquid pressure, 10 bara; reaction temperature, 120 °C.

Flow Flow Direction	a)	b)	c)
	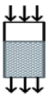	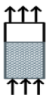	
X [%]	53	55	54
S_B [%]	67	66	67
S_T [%]	29	30	29

that the main oxygen transfer resistance was in the catalyst bed. This agreed with a permeation-transverse mass transfer effectiveness factor analysis, akin to internal-external mass transfer and reaction in a catalytic particle, which further provides guidance on catalyst choice and membrane reactor design. Scale-up of the microchannel reactor by an order of magnitude was demonstrated by increasing the width of the catalyst bed channel. The simple assembly of the flat membrane microchannel reactor suggests that other similar flat membranes could be used for scalable flow oxidation of organic compounds with molecular oxygen.

Acknowledgements

The assistance of Ian Briggs (Johnson Matthey) with ICP analysis is appreciated. Financial support by EPSRC, UK (grant EP/L003279/1) is gratefully acknowledged.

Appendix A. Supplementary data

Supplementary data to this article can be found online at https://doi.org/10.1016/j.cej.2018.10.023.

References

[1] T. Mallat, A. Baiker, Oxidation of alcohols with molecular oxygen on solid catalysts, Chem. Rev. 104 (2004) 3037–3058.
[2] C. Della Pina, E. Falletta, L. Prati, M. Rossi, Selective oxidation using gold, Chem. Soc. Rev. 37 (2008) 2077–2095.
[3] S. Caron, R.W. Dugger, S.G. Ruggeri, J.A. Ragan, D.H.B. Ripin, Large-scale oxidations in the pharmaceutical industry, Chem. Rev. 106 (2006) 2943–2989.
[4] R. Ciriminna, V. Pandarus, F. Béland, Y.-J. Xu, M. Pagliaro, Heterogeneously catalyzed alcohol oxidation for the fine chemical industry, Org. Process Res. Dev. 19 (2015) 1554–1558.
[5] H.P.L. Gemoets, Y. Su, M. Shang, V. Hessel, R. Luque, T. Noël, Liquid phase oxidation chemistry in continuous-flow microreactors, Chem. Soc. Rev. 45 (2016) 83–117.
[6] Z. Guo, B. Liu, Q. Zhang, W. Deng, Y. Wang, Y. Yang, Recent advances in heterogeneous selective oxidation catalysis for sustainable chemistry, Chem. Soc. Rev. 43 (2014) 3480–3524.
[7] M. Sankar, N. Dimitratos, P.J. Miedziak, P.P. Wells, C.J. Kiely, G.J. Hutchings, Designing bimetallic catalysts for a green and sustainable future, Chem. Soc. Rev. 41 (2012) 8099–8139.
[8] S.E. Davis, M.S. Ide, R.J. Davis, Selective oxidation of alcohols and aldehydes over supported metal nanoparticles, Green Chem. 15 (2013) 17–45.
[9] D.S. Mannel, S.S. Stahl, T.W. Root, Continuous flow aerobic alcohol oxidation reactions using a heterogeneous $Ru(OH)_x/Al_2O_3$ catalyst, Org. Process Res. Dev. 18 (2014) 1503–1508.
[10] A. Gavriilidis, A. Constantinou, K. Hellgardt, K.K. Hii, G.J. Hutchings, G.L. Brett, S. Kuhn, S.P. Marsden, Aerobic oxidations in flow: opportunities for the fine chemicals and pharmaceuticals industries, React. Chem. Eng. 1 (2016) 595–612.
[11] C.A. Hone, D.M. Roberge, C.O. Kappe, The use of molecular oxygen in pharmaceutical manufacturing: is flow the way to go? ChemSusChem 10 (2017) 32–41.
[12] X. Ye, M.D. Johnson, T. Diao, M.H. Yates, S.S. Stahl, Development of safe and scalable continuous-flow methods for palladium-catalyzed aerobic oxidation reactions, Green Chem. 12 (2010) 1180–1186.
[13] J.F. Greene, J.M. Hoover, D.S. Mannel, T.W. Root, S.S. Stahl, Continuous-flow aerobic oxidation of primary alcohols with a copper(I)/TEMPO catalyst, Org. Process Res. Dev. 17 (2013) 1247–1251.
[14] N. Zotova, K. Hellgardt, G.H. Kelsall, A.S. Jessiman, K.K. Hii, Catalysis in flow: the practical and selective aerobic oxidation of alcohols to aldehydes and ketones, Green Chem. 12 (2010) 2157–2163.
[15] A. Comite, A. Bottino, G. Capannelli, C. Costa, R. Di Felice, 4 – Multi-phase catalytic membrane reactors A2 – Basile, Angelo, Handbook of Membrane Reactors, Woodhead Publishing, 2013, pp. 152–187.
[16] X. Tan, K. Li, Membrane microreactors for catalytic reactions, J. Chem. Technol. Biotechnol. 88 (2013) 1771–1779.
[17] T. Noël, V. Hessel, Membrane microreactors: gas-liquid reactions made easy, ChemSusChem 6 (2013) 405–407.
[18] A. Constantinou, G. Wu, A. Corredera, P. Ellis, D. Bethell, G.J. Hutchings, S. Kuhn, A. Gavriilidis, Continuous heterogeneously catalyzed oxidation of benzyl alcohol in a ceramic membrane packed-bed reactor, Org. Process Res. Dev. 19 (2015) 1973–1979.
[19] H. Zhang, S.G. Weber, Teflon AF Materials, in: I.T. Horvath (Ed.), Fluorous Chemistry. Top. Curr. Chem. Springer-Verlag Berlin, Berlin, Heidelberg, 2012.
[20] T.P. Petersen, A. Polyzos, M. O'Brien, T. Ulven, I.R. Baxendale, S.V. Ley, The oxygen-mediated synthesis of 1,3-butadiynes in continuous flow: using teflon AF-2400 to effect gas/liquid contact, ChemSusChem 5 (2012) 274–277.
[21] M. Brzozowski, M. O'Brien, S.V. Ley, A. Polyzos, Flow chemistry: intelligent processing of gas-liquid transformations using a tube-in-tube reactor, Acc. Chem. Res. 48 (2015) 349–362.
[22] S.R. Chaudhuri, J. Hartwig, L. Kupracz, T. Kodanek, J. Wegner, A. Kirschning, Oxidations of allylic and benzylic alcohols under inductively-heated flow conditions with gold-doped superparamagnetic nanostructured particles as catalyst and oxygen as oxidant, Adv. Synth. Catal. 356 (2014) 3530–3538.
[23] G. Wu, A. Constantinou, E. Cao, S. Kuhn, M. Morad, M. Sankar, D. Bethell, G.J. Hutchings, A. Gavriilidis, Continuous heterogeneously catalyzed oxidation of benzyl alcohol using a tube-in-tube membrane microreactor, Ind. Eng. Chem. Res. 54 (2015) 4183–4189.
[24] J.F. Greene, Y. Preger, S.S. Stahl, T.W. Root, PTFE-membrane flow reactor for aerobic oxidation reactions and its application to alcohol oxidation, Org. Process Res. Dev. 19 (2015) 858–864.
[25] L. Yang, K.F. Jensen, Mass transport and reactions in the tube-in-tube reactor, Org. Process Res. Dev. 17 (2013) 927–933.
[26] D.I. Enache, J.K. Edwards, P. Landon, B. Solsona-Espriu, A.F. Carley, A.A. Herzing, M. Watanabe, C.J. Kiely, D.W. Knight, G.J. Hutchings, Solvent-free oxidation of primary alcohols to aldehydes using Au-Pd/TiO_2 catalysts, Science 311 (2006) 362–365.
[27] S. Meenakshisundaram, E. Nowicka, P.J. Miedziak, G.L. Brett, R.L. Jenkins, N. Dimitratos, S.H. Taylor, D.W. Knight, D. Bethell, G.J. Hutchings, Oxidation of alcohols using Supported Gold and Gold-Palladium Nanoparticles, Faraday Discuss. 145 (2010) 341–356.
[28] M. Sankar, E. Nowicka, R. Tiruvalam, Q. He, S.H. Taylor, C.J. Kiely, D. Bethell, D.W. Knight, G.J. Hutchings, Controlling the duality of the mechanism in liquid-phase oxidation of benzyl alcohol catalysed by supported Au-Pd nanoparticles, Chem. Eur. J. 17 (2011) 6524–6532.
[29] F. Galvanin, M. Sankar, S. Cattaneo, D. Bethell, V. Dua, G.J. Hutchings, A. Gavriilidis, On the development of kinetic models for solvent-free benzyl alcohol oxidation over a gold-palladium catalyst, Chem. Eng. J. 342 (2018) 196–210.
[30] G. Wu, G.L. Brett, E. Cao, A. Constantinou, P. Ellis, S. Kuhn, G.J. Hutchings, D. Bethell, A. Gavriilidis, Oxidation of cinnamyl alcohol using bimetallic Au-Pd/TiO_2 catalysts: a deactivation study in a continuous flow packed bed microreactor, Catal. Sci. Tech. 6 (2016) 4749–4758.
[31] M. Goethals, B. Vanderstraeten, J. Berghmans, G. De Smedt, S. Vliegen, E. Van't Oost, Experimental study of the flammability limits of toluene-air mixtures at elevated pressure and temperature, J. Hazard. Mater. 70 (1999) 93–104.
[32] E. Cao, M. Sankar, S. Firth, K.F. Lam, D. Bethell, D.K. Knight, G.J. Hutchings, P.F. McMillan, A. Gavriilidis, Reaction and Raman spectroscopic studies of alcohol oxidation on gold-palladium catalysts in microstructured reactors, Chem. Eng. J. 167 (2011) 734–743.
[33] E. Cao, M. Sankar, E. Nowicka, Q. He, M. Morad, P.J. Miedziak, S.H. Taylor, D.W. Knight, D. Bethell, C.J. Kiely, A. Gavriilidis, G.J. Hutchings, Selective suppression of disproportionation reaction in solvent-less benzyl alcohol oxidation catalysed by supported Au-Pd nanoparticles, Catal. Today 203 (2013) 146–152.
[34] J.J. Carberry, Chemical and Catalytic Reaction Engineering, McGraw-Hill, New York, 1976.